

Supporting Information

Multilayer nanoassembly of Sn-nanopillar arrays sandwiched between graphene layers for high-capacity lithium storage

Liwen Ji[†], Zhongkui Tan[†], Tevye Kuykendall[†], Eun Ji An[†], Yanbao Fu[‡], Vincent Battaglia[‡], and Yuegang Zhang^{†}*

[†] The Molecular Foundry, Lawrence Berkeley National Laboratory,

One Cyclotron Road, Berkeley, California 94720, USA.

[‡] Advanced Energy Technology Department, Lawrence Berkeley National Laboratory, One Cyclotron Road, Berkeley, California 94720, USA.

** E-mail: yzhang5@lbl.gov*

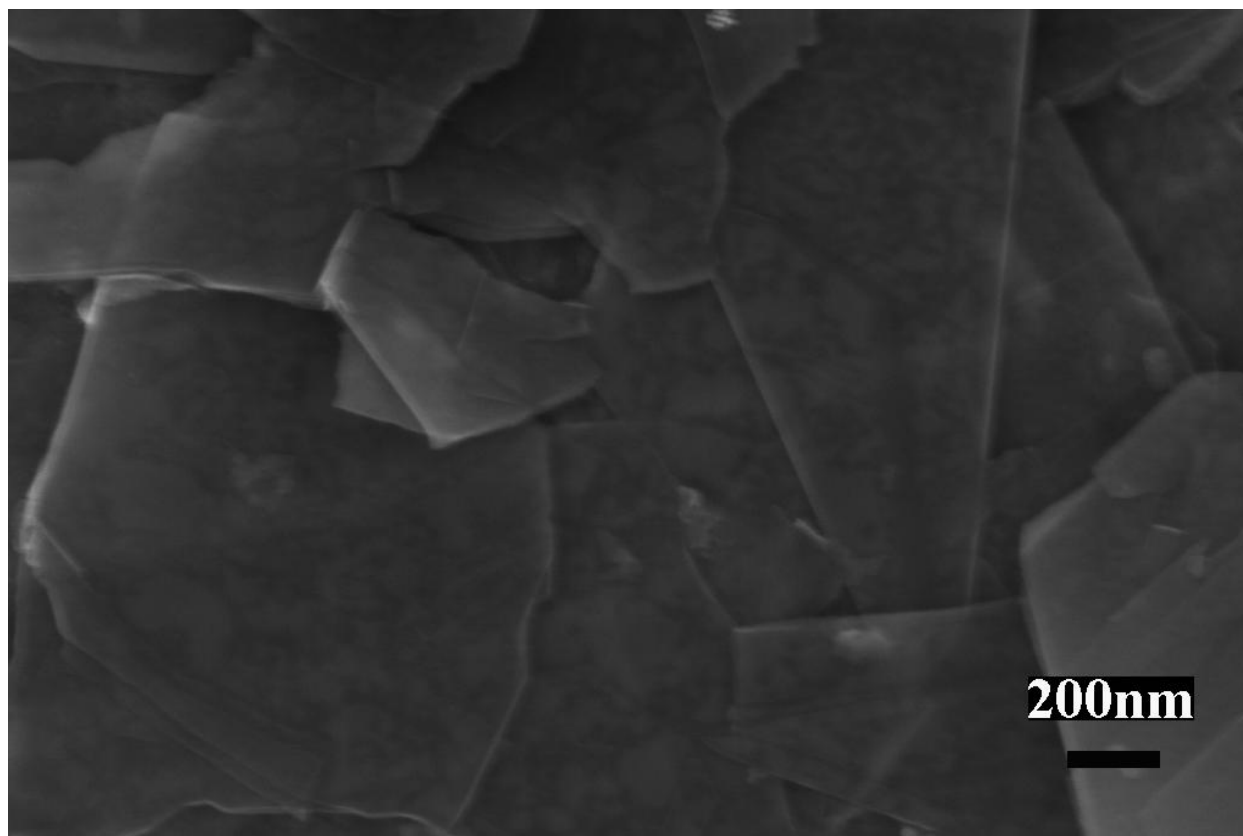


Fig. S1. SEM image of the exfoliated graphene films after filtration and transfer on Cu foil.

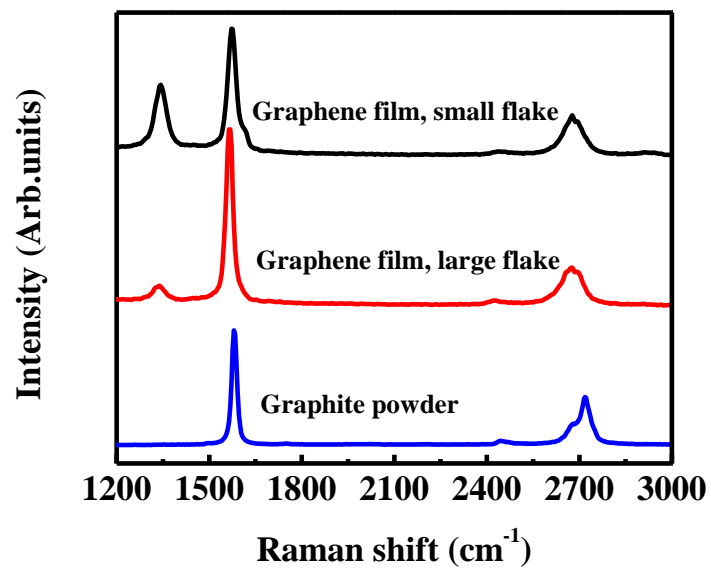


Fig. S2. Raman spectra of the exfoliated graphene films (composed with both large flakes and small flakes) and graphite powder.

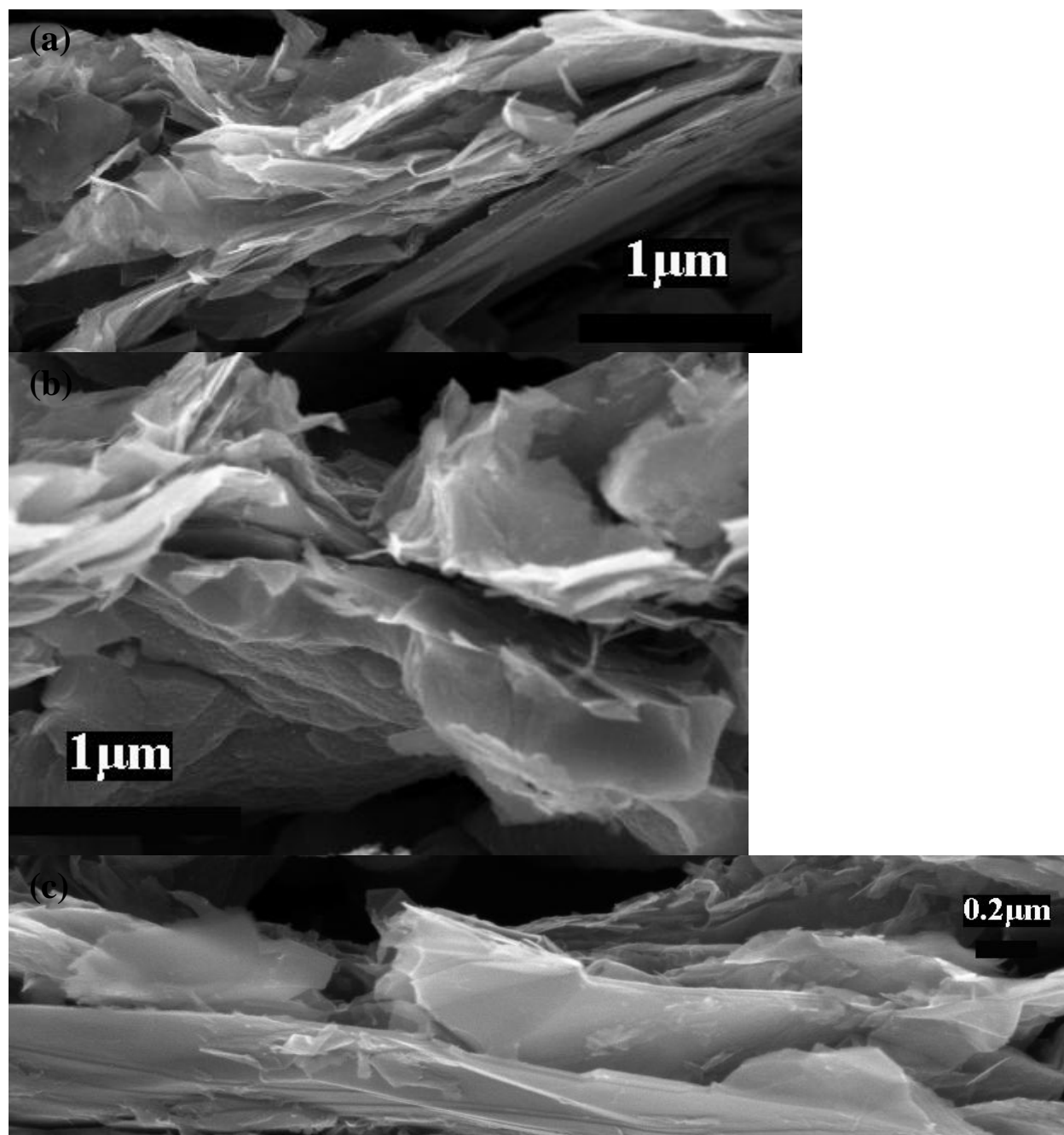


Fig. S3. Cross-sectional SEM images of multilayer graphene prepared via filtering liquid phase exfoliated graphene NMP solution with an average thickness of about 800-1200nm. Here, the volume of filtered solutions is 10 times of that in the main text, we make the conclusions that graphene films in graphene/Sn-nanopillar multilayered nanocomposite has the average thickness of about 100nm.

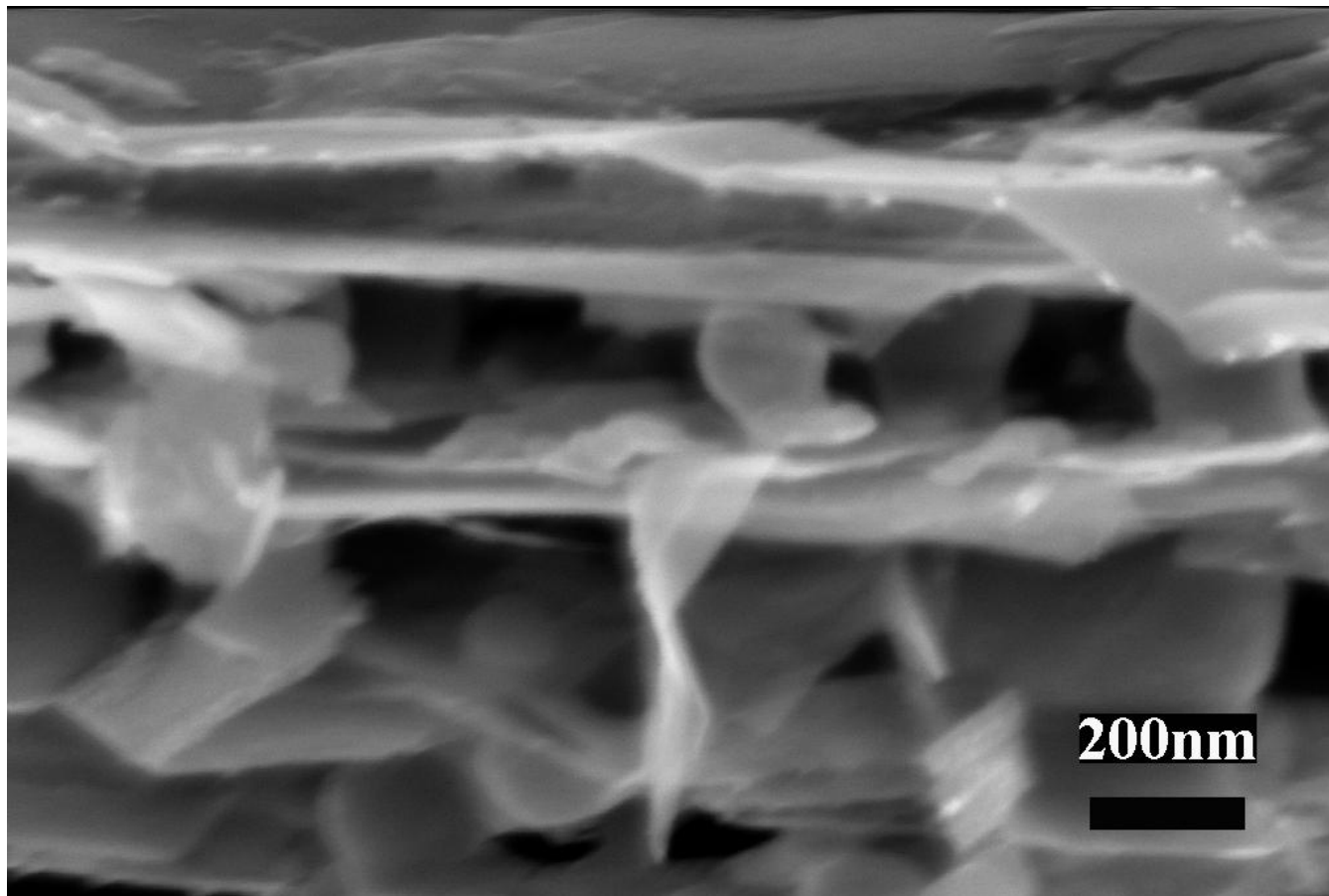


Fig. S4. Cross-sectional SEM images of graphene/Sn nanopillar multilayered nanocomposites where the thickness of graphene component is clearly shown (about 80-100nm).

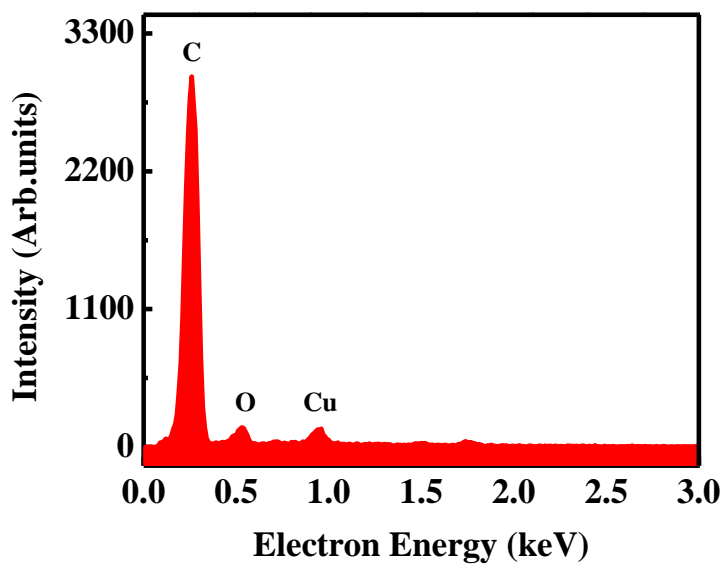


Fig. S5. SEM-EDX analysis of the pure graphene film on Cu foil. The large carbon peak prove the existence of graphene films, while the Cu and O impurities may come from Cu foil substrate the surface oxide of Cu foil substrate, respectively.

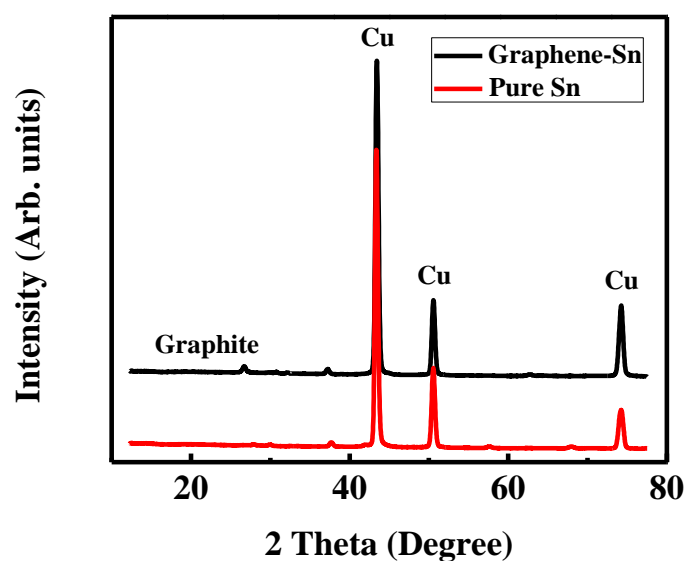


Fig. S6. WAXD patterns of the as-prepared graphene/Sn-nanopillar nanocomposites and the as-evaporated Sn films on Cu foils. WAXD patterns show clear peaks of the Cu substrates and small amount of graphite (residues due to incomplete exfoliation). We did not see any corresponding diffraction peaks of Sn components in both the graphene/Sn-nanopillar nanostructure and the thermally evaporated pure Sn films. Since Sn is indeed present in the sample as shown in Fig. S4, we can conclude that the nanosized Sn is in an amorphous phase.^[S1,S2]

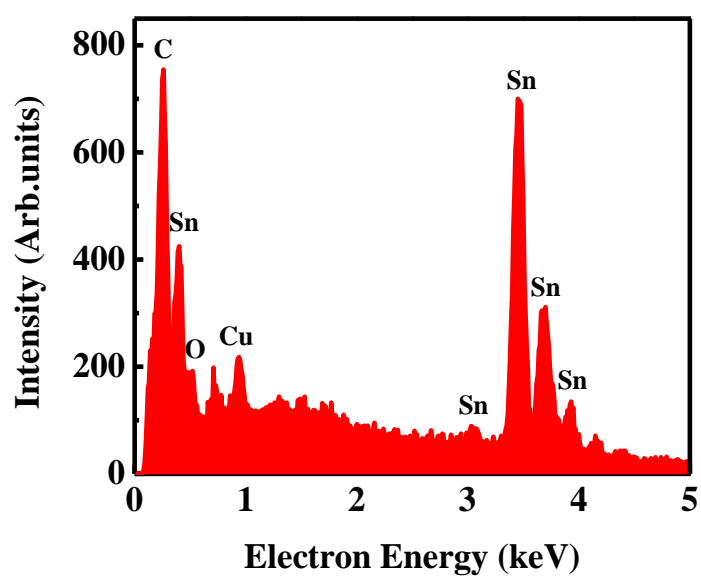


Fig. S7. SEM-EDX analysis of the multilayer graphene/Sn-nanopillar nanostructures. Clear peaks of Sn and C are identified in the graphene/Sn-nanopillar nanocomposites.^[S1-S3] In addition, a small contribution from oxygen at 0.53 keV suggests the presence of surface oxide impurities.

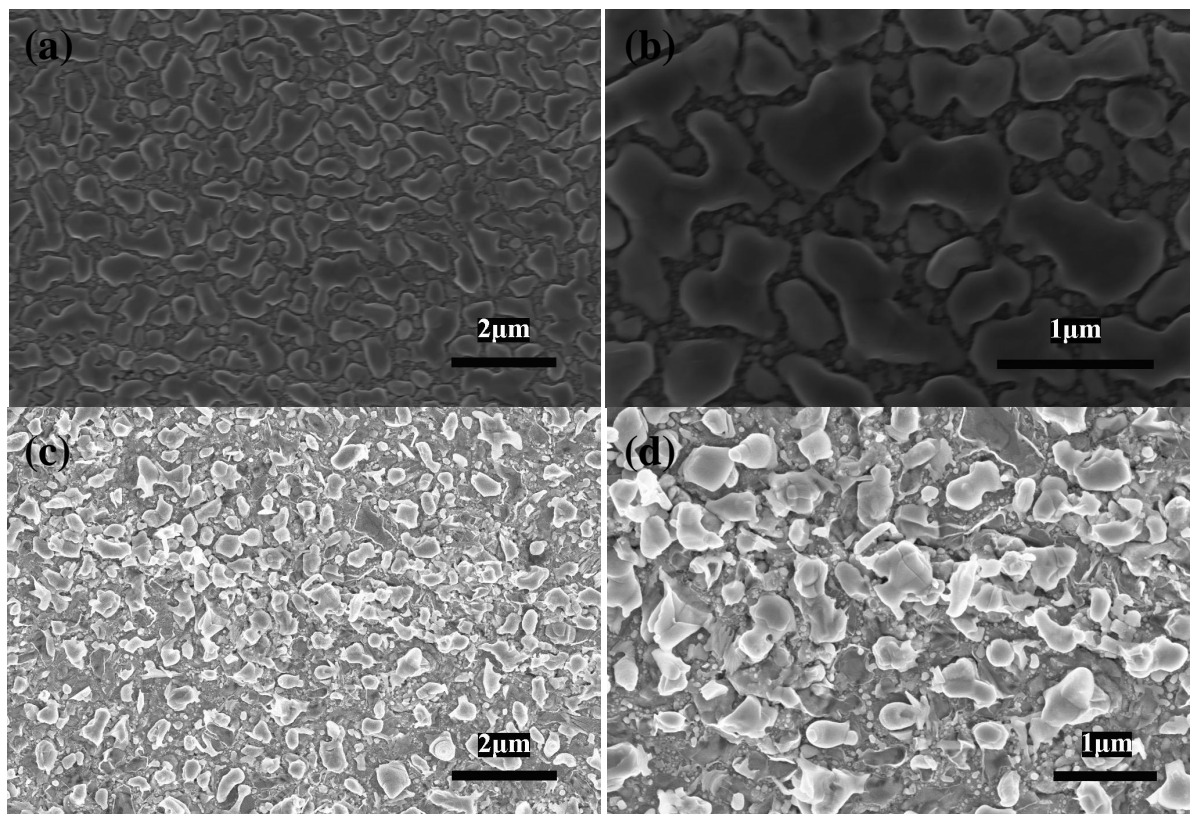


Fig. S8. SEM images of thermally evaporated Sn films directly on Cu foil, before (a,b) and after (c,d) further thermal annealing. No nanopillar structure is identified in these control samples.

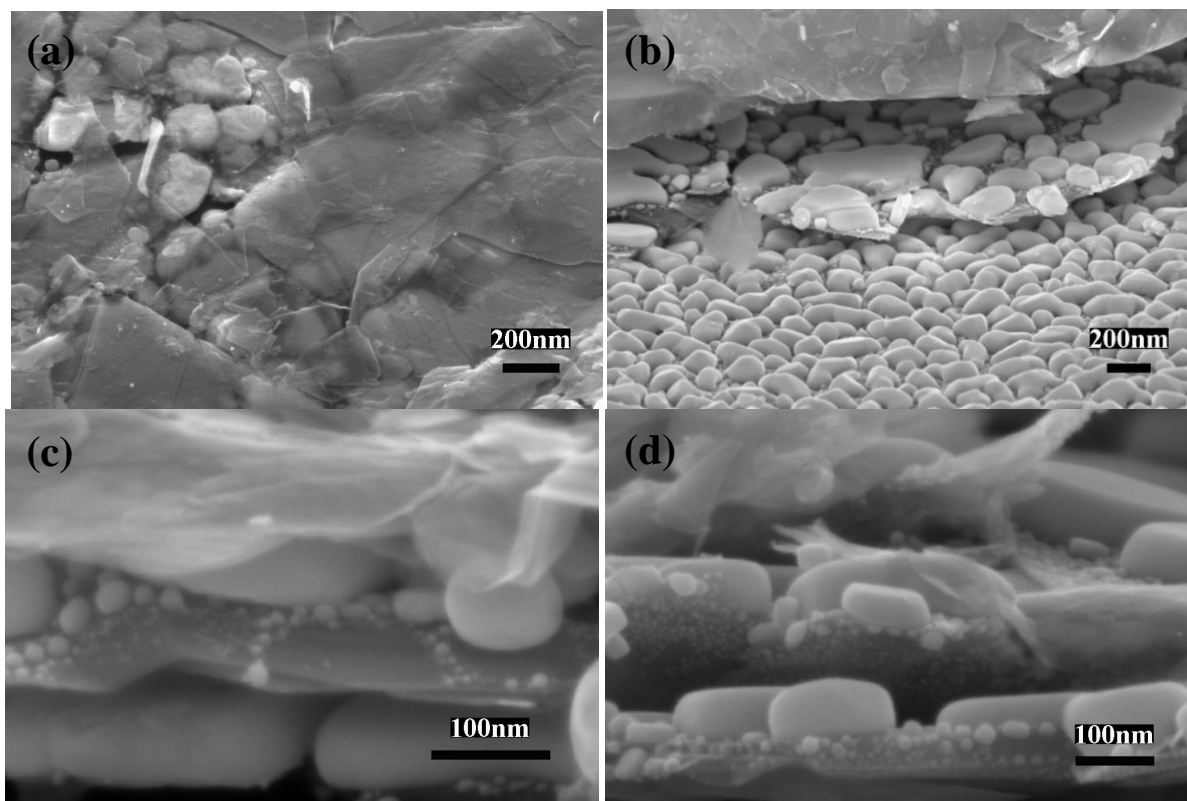


Fig. S9. SEM planar-views (a, b) and cross-sectional views (c, d) of the graphene/Sn multilayers films before thermal annealing process. The as-deposited Sn films show a low-aspect-ratio grainy structure typical for low-melting-point metal films deposited on non-wetting surfaces.

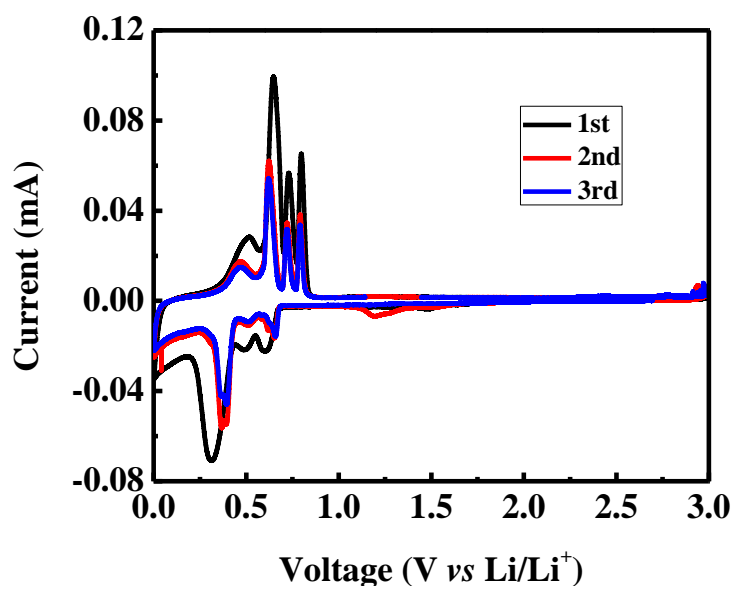


Fig. S10. CV curves of pure Sn films prepared by thermal evaporation.

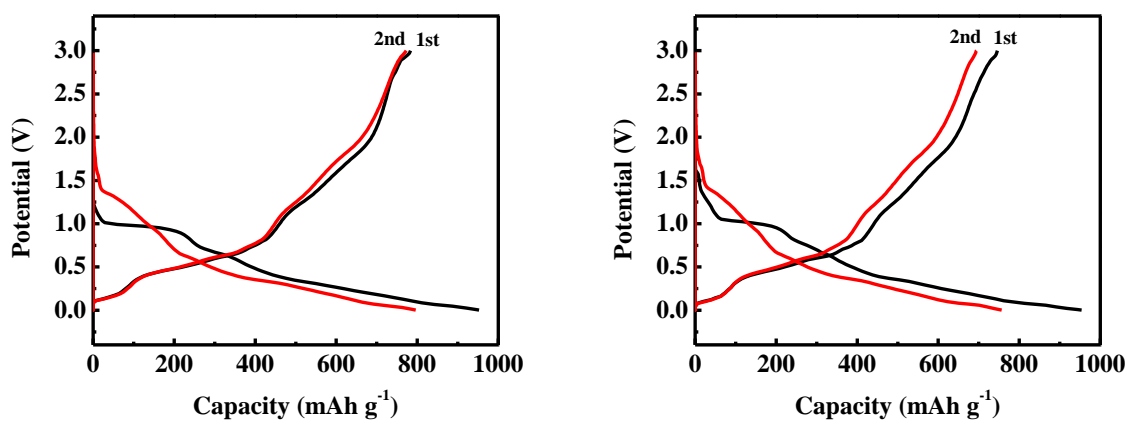


Fig. S11. Galvanostatic charge/discharge profiles of two additional half cells made from the graphene/Sn-nanopillar nanocomposites similar to those in Fig. 3 of the main text. The current density is 0.05 A g⁻¹; cutoff voltage window is 2 mV to 3.0 V.

Notes and references:

- (S1) M. Noh, Y. Kwon, H. Lee, J. Cho, Y. Kim, and M. G. Kim, *Chemistry of Materials*, 2005, **17**, 1926.
- (S2) M. Marcinek, L. J. Hardwick, T. J. Richardson, X. Song, and R. Kostecki, *Journal of Power Sources*, 2007, **173**, 965.
- (S3) B. Veeraraghavan, A. Durairajan, B. Haran, B. Popov, R. Guidotti, *Journal of The Electrochemical Society* 2002, **149**, A675-A681.